ISSN 1392–1320 MATERIALS SCIENCE (MEDŽIAGOTYRA). Vol. 25, No. 4. 2019

Electrolytic Preparation of Al-Sm Alloy in SmF_3-LiF-Sm_2O_3 Molten Salt System

Xiaolian ZHANG, Chubin YANG *, Hongxia LIU, Guanghuai PENG

Jiangxi Provincial Engineering Research Center for Magnesium Alloy, Gannan Normal University, Ganzhou 341000, PR China

crossref http://dx.doi.org/10.5755/j01.ms.25.4.20437

Received 27 March 2018; accepted 10 July 2018

In the present paper, an Al rod as liquid cathode was added into the SmF_3-LiF-Sm_2O_3 molten salt system and subsequently the Al-Sm alloy was prepared by the liquid cathode electrolysis method. The effects of electrolysis temperature, cathode current density and electrolyte composition on the current efficiency were studied. The results demonstrated that the maximum content of Sm in the Al-Sm interalloy could reach up to 32.8 wt.%, whereas the alloy was mainly composed of the Al substrate, Al_4Sm and Al_3Sm phases. The current efficiency increased first subsequently decreased as the electrolysis temperature and cathode current density increased. Simultaneously, the electrolyte composition had a high impact on the current efficiency. When the mass ratio of $SmF_3$and LiF was 4, the current efficiency was 62.8 %.

Keywords: molten salt electrolysis, Al-Sm interalloy, current efficiency.

1. INTRODUCTION

The rare earth element Samarium (Sm) is a white metal that is currently mainly utilized in samarium cobalt magnetic materials [1]. Also, the applications of Sm in other areas have also been developed, such as in Sm enhancing the performance of magnesium alloys through the solid solution strengthening mechanism, since the solid solubility of Sm in magnesium can reach up to 5.8 wt.% [2, 3]. Currently, the Sm that is added into an alloy substrate is mainly accomplished through the reduction of samarium oxide by the metallic lanthanum (La). This process, however, has low output, complicated equipment, discontinuous operation, high energy consumption and cost. Therefore, in recent years, researches on the low-cost electrolysis for Sm and the corresponding alloys have gradually been focused on.

The current studies indicated that the electrolytic preparation of Sm includes two stages [4]:

$$Sm^{3+} + e \rightarrow Sm^{2+}; \quad (1)$$

$$Sm^{2+} + 2\,e \rightarrow Sm. \quad (2)$$

In contrast, the element Sm cannot be directly obtained from the aforementioned electrolysis process since the reduction potential of Sm^{2+} in step (2) was significantly negative than the reduction potential of Li^+ in the molten salt. Therefore, the electrolysis process is mainly utilized in the Sm-containing interalloy preparation. The Al-Sm interalloy was prepared in the LiCl-KCl molten salt [5]. It also can reduced Sm_2O_3 directly in the LiCl-KCl-AlCl3 molten salt system through an electrochemical method, consequently obtaining an Al-Sm interalloy [6]. In contrast, during the electrolysis, due to the strong hygroscopicity and higher volatility of $RECl_3$(RE: the rare earth element), the high solubility of rare earths in the molten salt system, the pollution of chlorine generated by electrolysis, the low current efficiency and the low output of metals, the electrolysis system with RECl3 is gradually replaced by the electrolysis system with fluoride [7]. It was pointed out that the Al-Sm interalloys prepared through electrolysis in the LiF-CaF_2-Sm_2O_3-AlF_3 system are mainly composed of Al, Al_2Sm and Al_3Sm phases [8]. The molten melt density was measured and operation conditions were optimized to separate Al-Sm alloy product from the fluoride molten melt electrolysis media based on density differences [9]. The cathodic reduction behavior of Sm ions in the LiF-CaF_2 system was also investigated in [10]. It could be observed that the current researches mainly focused on the electrochemical reduction mechanism of Sm ions, whereas a significant lack of study on electrolysis exists, especially on the electrolysis in the SmF_3-LiF-Sm_2O_3 molten salt system.

Based on the research status, in this study the SmF_3-LiF fluoride molten salt system was adopted and the aluminum and samarium oxides were utilized as raw materials for the Al-Sm alloy preparation through the liquid cathode method, which significantly reduced the production cost and energy consumption. In addition, the affecting roles of electrolyte composition, electrolysis temperature and current density on the current efficiency were investigated. The study could provide an experimental basis to the electrolysis of Al-Sm alloys, being of a significant industrial application value.

2. EXPERIMENT PROCEDURE

The experimental equipment is presented in Fig. 1. In the present paper, the SmF_3-LiF-Sm_2O_3 was utilized as the electrolyte. Anhydrous SmF3 (99.9 %), LiF(≥ 99 %) and Sm_2O_3(99.5 – 99.9 %) were purchased from Jiangxi Ganfeng Lithium Co., Ltd.

* Corresponding author.Tel./fax: +86 23 65102821.
E-mail address: *yangchubin831012@163.com* (C.B. Yang)

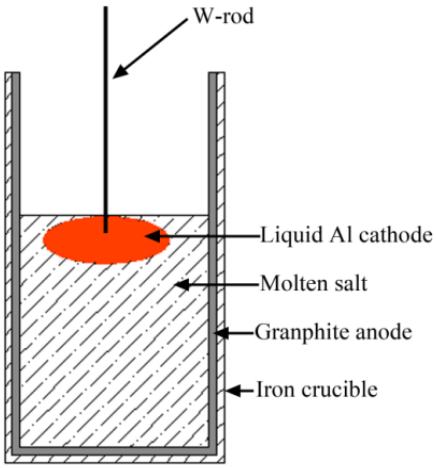

Fig. 1. Diagram of experimental equipment

The total mass of SmF_3 and LiF was 100g with various proportions. The weighed SmF_3 and LiF were stirred uniformly with a clean spatula and consequently introduced in an graphite crucible (Φ170 × 248 mm) which placed into an iron crucible (Φ190 × 250 mm), as shown in Fig. 1. The crucible was heated to a certain temperature for the raw materials to be melted in a resistance furnace, and following the Sm_2O_3 (50 g) was added and stirred. Subsequently an aluminum rod (≥ 99 %) with a mass of 50 g was added. Following the aluminum rod melting, the tungsten rod of 6.0 mm diameter was insert to the liquid aluminum as a conducting medium, and the electrolysis began with the liquid aluminum as cathode and the graphite with the diameter of 120 mm as anode. The electrolysis duration was 30 min. The composition of electrolyte such as the electrolysis temperature and cathode current density was changed for the study on electrolysis to be performed.

The microstructure of the electrolytic Al-Sm interalloy was observed by Scanning Electron Microscopy (SEM) and the phase composition was confirmed by Energy Dispersion Spectrum (EDS) and X-ray Diffraction (XRD).

3. RESULTS AND DICUSSION

3.1. Microstructure of Al-Sm interalloy prepared through electrolysis

Fig. 2 presents the SEM images of Al-Sm interalloys with various contents of Sm, among which Fig. 2 a and b represented the Al-21.7 wt.% Sm, whereas Fig. 2 c and d represented the Al-32.8 wt.% Sm. It could be observed from Fig. 2 that the interalloy was mainly composed of the black substrate and a high amount of white phases. The white secondary phase existed in two morphologies, the wheat-like coarse phase and the needle-like fine phase.

The EDS characterization was executed for all phases in the Al-Sm interalloy (arrows in Fig. 2 d). The results are presented in Table 1. As it could be observed from the EDS result, the white phase was an Al-Sm mesophase, containing a high amount of Sm, whereas the black substrate was mainly composed of Al. According to the EDS energy spectrum results, the Al/Sm atomic ratio of the wheat-like grain was approximately 4, whereas the Al/Sm atomic ratio of the needle-like phase was approximately 3.

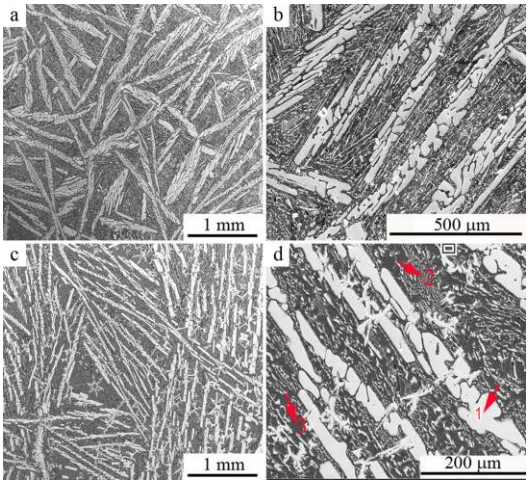

Fig. 2. a, b – SEM images of Al-21.7 % Sm; c, d – SEM images of Al-32.8 %Sm

Table 1. EDS result of corresponding positions in Fig. 2 d

Position	Al		Sm	
	wt.%	at%	wt.%	at%
Point 1	43.75	81.25	56.25	18.75
Point 2	40.87	75.34	59.13	24.66
Point 3	99.24	99.86	0.76	0.14

In order to further confirm the phase composition of the Al-Sm interalloy, the XRD diffraction analysis was executed on the sample and the obtained patterns are presented in Fig. 3.

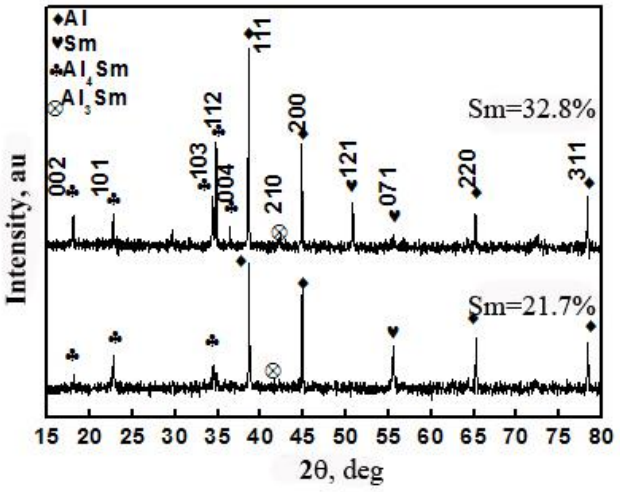

Fig. 3. XRD diffraction patterns of Al-Sm

According to the XRD pattern, the Al-Sm interalloy consisted mainly of Al, Al_4Sm and Al_3Sm phases. As the Sm content increased, the Al4Sm diffraction peak became intensified, indicating a higher content of Al_4Sm phase. At present, a high number of studies have demonstrated that, either in the fluoride salt or the chloride salt, the Al_3Sm phase will form during the electrolysis, whereas the Al_4Sm phase is relatively rare [10]. This occurs mainly because the Al_4Sm phase formation temperature is significantly high, whereas the general electrolysis temperature is quite lower than the corresponding formation temperature. It

could obtain significantly fine Al_4Sm whiskers when electrolyzed the LiCl-KCl-$SmCl_3$ molten salt at 773 K for 5 hours [5]. It was suggested that the Al_4Sm phase was formed in the local regions of the surface, since the temperature in the local regions could increase to 1500K or higher. However, the Al_4Sm phase in the LiCl-KCl-$AlCl_3$-Sm_2O_3 molten salt system by a constant current electrolysis at the low temperature of 773 K was also obtained in [11]. These results indicated that the Al_4Sm phase formation was not only related to the electrolysis temperature, whereas also to the electrolyte composition. In this experiment, the electrolysis temperature was relatively high (> 1000 K) and the SmF_3-LiF-Sm_2O_3 was adopted as the electrolyte, which might be conducive to the Al_4Sm phase formation.

3.2. Sm content and current efficiency for electrolysis under various conditions

Table 2 lists the Sm contents in Al-Sm alloys prepared by electrolysis at various process conditions. As it could be observed from Table 2, the content of Sm in the interalloy could reach up to the maximum of 32.8 wt.%, whereas the lowest content was 21.7 wt.%. According to the Sm content obtained by electrolysis and the electrolysis process parameters, the current efficiency could be calculated by Eq. 3 and the results are presented in Table 2.

$$\eta = \frac{m_0}{kIt} \times 100\%, \tag{3}$$

where m_0 is the content of Sm in the electrolytic product in g; k is the electrochemical equivalent of Sm in g/C; I is the electrolytic current in A; t is the electrolysis duration in h.

The current efficiency is one of the key parameters to evaluate the quality of electrolysis. It constitutes a significantly complicated process since it is dependent on the comprehensive action of several process parameters of electrolysis. In this experiment, the addition of Al rod as a liquid sate cathode had a strong reducibility, therefore the reduction reaction presented in Eq. 4 and Eq. 5 might occur, such as the Sm^{3+} in SmF_3 and the Sm_2O_3 might be reduced to metallic Sm by Al. Therefore, the calculated current efficiency, as presented in Table 2, might be not simply an electrolytic current efficiency, whereas it could contain the current efficiency including the aluminothermic reduction.

$$Al(l) + SmF_3(l) \rightarrow Sm(s) + AlF_3(s); \tag{4}$$

$$2Al(l) + Sm_2O_3(l) \rightarrow 2Sm(s) + Al_2O_3(s). \tag{5}$$

For the Eq. 4 and Eq. 5 right proceeding confirmation, a thermodynamic calculation was necessary [12]. The thermodynamic parameters of every substance at various temperatures are listed in Table 3. The Gibbs free energy is calculated as:

$$\Delta G = \Delta H - T\Delta S, \tag{6}$$

where ΔH is the enthalpy change of the reaction, $KJ \cdot mol^{-1}$; ΔS is the entropy change, $J \cdot K^{-1} \cdot mol^{-1}$; T is the reaction temperature, K. The thermodynamic parameters in Table 3 were substituted into Eq. 6 and consequently the calculated $\Delta G > 0$. Therefore, the thermal reduction reactions, presented in Eq. 4 and Eq. 5 at the electrolysis temperature, did not occur, therefore the calculated current efficiency, presented in Table 2, was the electrolytic current efficiency.

As it could be observed from Table 2, the current efficiency was closely related to the electrolysis temperature, the current density and the composition of the electrolyte. The current efficiency in the electrolysis increased first and subsequently decreased as the electrolysis temperature increased, leading to the best current efficiency at 1020 °C, as presented in Fig. 4 a. This mainly resulted from the significantly low electrolysis temperature leading to lower electric conductivity of the molten salt. In addition, the molten salt viscosity at the low temperature increased, subsequently the surface tension of the molten salt increased, resulting in the insufficient separation of the liquid sate metal and the electrolyte interface, along with a lower current efficiency. In contrast, when the electrolysis temperature was too high, the rare earth metal (REM) solubility in the molten salt increased correspondingly. The REM dissolved in the molten salt could react with oxygen, water, carbon dioxide and graphite, causing a REM significant loss, thereby drastically reducing the current efficiency. Therefore, the significantly low and high electrolysis temperatures are both adverse to the current efficiency.

When the cathode current density was too high, the cathode area would be heated, which increased the metal dissolution possibility, leading in alkali metal ions to be easily reduced and result in a lower current efficiency. When the cathode current density was low, the metal precipitation rate decreased, therefore the corresponding dissolution rate increased, reducing the current efficiency also. This was consistent with the results of the experiment, as presented in Fig. 4 b. The ratio change of SmF_3 and LiF could adjust the solubility of Sm(III) ions in the molten salt, consequently affecting the Sm-Al alloy deposition rate on the cathode, as presented in Fig. 4 c. Although the affecting rule of electrolysis parameters on the current efficiency in the SmF_3-LiF-Sm_2O_3 molten salt system was rarely reported, it was systematically studied in other electrolysis systems. The effect of electrolysis process parameters on the current efficiency in the electrolytic preparation of Mg/Li and Mg/Zr alloys and obtained the affecting rule similarly to this paper in [13]. Therefore, regarding the preparation of various alloys in various molten salt systems, the electrolysis process parameters were required to be studied systematically in order for the optimum conditions to be obtained. This proved a promising method that could provide guidance for industrial production processes.

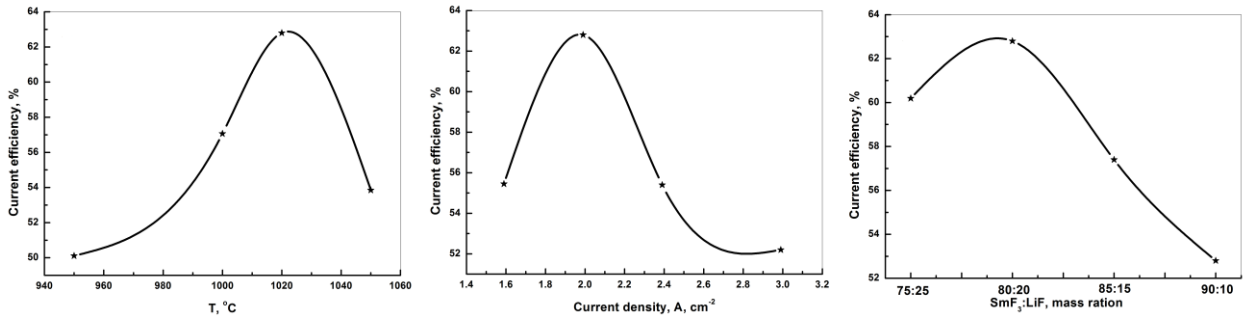

a b c

Fig. 4. Effects of electrolysis process parameters on current efficiency: a – electrolysis temperature; b – cathode current density; c – electrolyte composition

Table 2. Sm content and current efficiency under various electrolysis processes

I/A	T, ℃	SmF_3:LiF	Al-Sm/g	Sm, %	Al, %	η
100	950	80:20	196.85	23.8	Bal.	50.11
100	1000	80:20	203.35	26.2	Bal.	57.06
100	1020	80:20	208.72	28.1	Bal.	62.8
100	1050	80:20	200.35	25.1	Bal.	53.85
100	1020	75:25	206.28	27.3	Bal.	60.19
100	1020	85:15	203.67	26.4	Bal.	57.4
100	1020	90:10	199.37	24.8	Bal.	52.8
80	1020	80:20	191.48	21.7	Bal.	55.45
120	1020	80:20	212.16	29.3	Bal.	55.4
150	1020	80:20	223.21	32.8	Bal.	52.2

Table 3. Thermodynamic parameters of various materials at certain temperature

Parameter	T/K	Al	Al_2O_3	AlF_3	Sm	SmF_3	Sm_2O_3
H, $KJ.mol^{-1}$	1200	37.31	-1572.17	-1422.7	36.15	-1565.18	-1706.5
	1400	43.66	-1546.25	-1401.91	42.96	-1537.67	-1675.62
S, $J.K^{-1}.mol^{-1}$	1200	79.47	202.97	198.06	114.52	271.07	339.1
	1400	84.36	222.94	214.08	119.87	292.23	362.9

4. CONCLUSIONS

In this paper, the Al-Sm alloy was prepared by the liquid state cathode electrolysis in the SmF_3-LiF-Sm_2O_3 molten salt system through the Al bar addition and the electrolysis control. The main conclusions were as follows:

1. When the SmF_3:LiF was 4:1, the electrolysis temperature was 1020 °C, the cathode current was 100 A and the electrolysis duration was 30 min, whereas the current efficiency reached the maximum value (62.8 %).
2. The content of Sm in the Al-Sm interalloy alloy could reach up to 32.8 wt.%. The phase in Mg-Sm interalloy was mainly composed of Al and Al-Sm intermetallic compounds.

Acknowledgments

This work was supported by the National Natural Science Foundation of China (No. 51464002).

REFERENCES

1. **Krishnan, M., Predeep, P., Rao, D.V., Sridhara Prajapat, C.L., Singh, M.R., Barshilia Harish, C., Chowdhury, P.** High coercivity Sm-Co thin films from elemental Sm/Co multilayer deposition and their microstructural aspects *Journal of Magnetism and Magnetic Materials* 430 2017: pp. 47 – 51. https://doi.org/10.1016/j.jmmm.2017.01.056
2. **Li, K.J., Li, Q.A., Jing, X.T., Jun, C., Zhang, X.Y., Zhang, Q.** Effects of Sm addition on microstructure and mechanical properties of Mg-6Al-0.6Zn alloy *Scripta Materialia* 60 (12) 2009: pp. 1101 – 1104. https://doi:10.1016/j.scriptamat.2009.02.048
3. **Li, Q.A., Zhang, Q., Wang, Y.G., Zhou, W.** Effects of Sm addition on microstructure and mechanical properties of a Mg-10Y alloy *China Foundry* 11 (1) 2014: pp. 28 – 32.
4. **Castrillejo, Y., Fernández, P., Medina, J., Hemández, P., Barrado, E.** Electrochemical extraction of samarium from molten chlorides in pyrochemical processes *Electrochimica Acta* 56 (24) 2011: pp. 8638 – 8644. https://doi:10.1016/j.electacta.2011.07.059
5. **Ji, D.B., Yan, Y.D., Zhang, M.L., Li, X., Jing, X.Y., Han, W., Xue, Y., Zhang, Z.J., Hartmann, T.** Electrochemical preparation of Al–Sm intermetallic compound whisker in LiCl–KCl Eutectic Melts *Electrochimica Acta* 165 2015: pp. 211 – 220. https:// doi:10.1016/j.electacta.2015.02.227

6. **Xue, Y., Wang, Q., Yan, Y.D., Zhang, Z.J.** Direct electrochemical reduction of Sm2O3 and formation of Al-Sm alloys in LiCl-KCl-AlCl3 melts *Chinese Journal of Inorganic Chemistry* 29 (9) 2013: pp. 1947 – 1951. https:// doi:10.3969/j.issn.1001-4861.2013.00.282
7. **Gibilaro, M., Massot, L., Chamelot, P., Taxil, P.** Study of neodymium extraction in molten fluorides by electrochemical co-reduction with aluminium *Journal of Nuclear Materials* 382 (1) 2008: pp. 39 – 45. https:// doi:10.1016/j.jnucmat.2008.09.004
8. **Gao, Y., Shi, Y.K., Liu, X.L., Huang, C., Li, B.** Cathodic Behavior of Samarium(III) and Sm-Al alloys Preparation in Fluorides Melts *Electrochimical Acta* 190 2016: pp. 208 – 214. https:// doi:10.1016/j.electacta.2015.12.117
9. **Jiao, Y.F., Wang, X., Liao, C.F., Su, J., Tang, H., Cai, B.Q., Sun, Q.C.** Density of Na3AlF6-AlF3-LiF-MgF2-Al2O3-Sm2O3 molten salt melt for Al-Sm alloy *Journal of Rare Earths* 36 (2) 2018: pp. 190 – 196. https://doi:10.1016/j.jre.2017.05.007
10. **Massot, L., Chamelot, P., Taxil, P.** Cathodic behaviour of samarium(III) in LiF–CaF2 media on molybdenum and nickel electrodes *Electrochimical Acta* 50 (28) 2005: pp. 5510 – 5517. https:// doi:10.1016/j.electacta.2005.03.046
11. **Liu, K., Liu, Y.L., Yuan, L.Y., He, H., Yang, Z.Y., Zhao, X.L., Chai, Z.F., Shi, W.Q.** Electroextraction of samarium from Sm_2O_3 in chloride melts *Electrochimical Acta* 129 2014: pp. 401 – 409. https:// doi:10.1016/j.electacta.2014.02.136
12. **Zhou, S.H., Napolitano, R.E.** Modeling of thermodynamic properties and phase equilibria for the Al-Sm binary system *Metallurgical and Materials Transactions A* 39 2008: pp. 502 – 512. https:// doi:10.1007/s11669-007-9022-0
13. **Chen, Z.** The research on Mg-Li and Mg-Zr alloys preparation by electrolysis in molten salt. PhD thesis, Harbin Engineering University, China, 2008: pp. 53 – 95.